Atomic diffusion in the FeAl alloy: A research via the kinetic Monte Carlo method

Erich Víctor MANRIQUE CASTILLO[*] and Felipe Américo REYES NAVARRO

Universidad Nacional Mayor de San Marcos, Facultad de Ciencias Físicas, Calle Germán Amézaga N° 375, Ciudad Universitaria, Lima, 01, Perú

*Corresponding author e-mail: emanriquec@unmsm.edu.pe

Abstract

For a binary alloy with an ordered structure B_2, we research the atomic migration by means of kinetic Monte Carlo simulations, where the atomic migration results from the exchange of positions between an atom and a vacancy in a rigid lattice. The atomistic kinetic model we used is based on the jump rate theory and the residence time algorithm, wherein we consider the pair interactions between neighbours up to the next-nearest neighbours. Likewise, we determine the ratio of the diffusion coefficients as a function of temperature and investigate the antiphase boundary mobility in the last stages of the ordering process. Furthermore, we calculate the autocorrelation function, which reveals that, in the lattice, not only the vacancy makes highly correlated jumps at low temperatures but the atoms jump to positions of their sub-lattice at moderate temperatures.

1. Introduction

The physical properties of technologically important materials originate in the reactions and processes to which they are subjected. In these materials, the atomic diffusion plays a key role because it is relevant to the kinetics of many microstructural changes occurring during preparation, processing and thermal treatment of the materials previously mentioned.

For example, there is currently a theoretical interest in superalloys, which have applications ranging from aircraft turbine engines to high speed drill bits. Specifically, for superalloys, it is sought to understand the different mechanisms of diffusion occurring through their respective volumes. Superalloys, such as FeAl, are interesting materials because they are resistant to high temperatures, maintain their structural and surface stability; besides, under high tensions and severe environments, their physical properties are majorly unchanged [1]. Superalloys are often rich in at least one of the following components: iron, nickel, cobalt, titanium and niobium.

The mechanical properties of superalloys are mainly determined by the microstructure acquired during the processing of the alloy. This microstructure can be greatly affected by changing the process variables such as alloy composition, temperature and annealing time. In many crystalline materials, the basic process of diffusion corresponds to the exchange of positions between a vacancy and a neighbouring atom.

Whereas atomic diffusion is well understood in simple metals, it is still not well comprehended in the B_2-ordered intermetallic alloys [2-4]. The B_2 structure, also called CsCl, has a body-centred cubic lattice and is of great attention scientific as well as technological [5]. Consequently, it is important to focus on the diffusion in the AB intermetallic with a crystal structure B_2, whose components have an electronic structure so that A belongs to column VIIIA and B, to column IIIB (FeAl, CoGa). Particularly, herein we will investigate the FeAl alloy.

Despite the diffusion mechanism in the B_2 phase is still controversial, it is accepted that the diffusion proceeds via the vacancy migration. The more reliable experimental information so far was achieved by using quasi-elastic Mossbauer spectroscopy (QEMS), which gives access to the individual jump vectors after a suitable modelling [6-9].

From experiments in ordered FeAl, it is commonly accepted that both diffusion occurs via jumps to the nearest neighbours (NNs) and the long-range order (LRO) is not altered during the vacancy migration. All this has encouraged some authors to suggest that atomic diffusion concretely results

from the sequence of highly correlated jumps of the vacancy. Consequently, two major categories of mechanisms have been proposed to explain how the energy barriers operating against diffusion can be overcome, without altering the LRO in the type-B_2 ordered alloys.

The first type of mechanism involves jumps to the next-nearest neighbours (NNNs). For instance, Donaldson et al. studied the diffusion of the nickel atoms in the B_2 compound NiGa; Lutze et al., the diffusion of [114]In in the B_2 compound NiAl; and Hahn et al., the self-diffusion in the B_2 intermetallic compound PdIn [10-12]. The second type of mechanism refers to cyclic movements wherein the atoms make a series of jumps to the NNs following a defined path. Typical examples are the six-jump cycle (6JC) [13-14], the anti-structure bridge mechanism [15], the triple-defect diffusion mechanism [16-18] and the 6JC assisted by antisites [19]. Likewise, several mechanisms additional to the 6JC have been postulated to describe the diffusion in the B_2 intermetallic compounds. However, most of those mechanisms, relevant to more complex alloys containing many point defects, are non-stoichiometric and are partially ordered [13,16,19].

2. Theoretical framework

2.1 Theory of diffusion

It is a process that can occur in two different ways. The first one is called transport diffusion, which occurs in the presence of a gradient of molecular concentration. That is, there is a net flow of matter, provoked by the random motion of atoms (and molecules), what results in a drop of the energy of the system. This flow is more frequent from a region of high concentration (high energy) to a region of low concentration (low energy). The process of diffusion will continue until the total energy of the system is minimized, resulting in a uniform distribution of atoms. A typical example of the use of diffusion occurs during the manufacture of semiconductors, which are required by the electronics industry.

The second one is called self-diffusion or tracer diffusivity, which doesn't constitute itself a net flux of matter. Tracer diffusivity occurs when labeled molecules move within a set of unlabeled molecules, all of them having identical properties; furthermore, we must point out that the overall concentration must be necessarily a constant value (overall concentration includes labeled and unlabeled molecules) [20,21]. Likewise, it should also be taken into account that the diffusivity of the labeled and unlabeled molecules depend on the total concentration and not on the number of labeled molecules. Usually, the labeled molecules, also known as tracers, are the isotopes of the atoms or molecules being studied. Besides, the pulsed-field gradient NMR can be used to experimentally measure self-diffusion. Even more, by using atomistic simulations along with the Einstein relation, see Eq. (6) below, self-diffusion can be calculated. Additionally, we also can affirm that, in a homogeneous material, self-diffusion is complicated to detect because of random movement of atoms; consequently, the number of atoms moving in any direction is equal.

The equations governing the atomic motion, which is characterized by the J flow, are the Fick's laws [22]. These laws represent a continuous and purely phenomenological description of the process of diffusion. The derivation of Fick's laws relies on continuous diffusion equations; however, Fick's laws can also be obtained from atomistic random jump models, namely, by using the propagator as a connection to the continuous theory. Thus, for a porous solid, the transport diffusion coefficient, which appears in the Fick's first law, and the self-diffusion coefficient, from the mean square displacement, coincide only at low concentrations of guest molecules. At this juncture, we want to thank two anonymous referees for contributing to better this paragraph as well as the two earlier.

The reactions and processes important in the treatment of alloys, which determine their microstructure, are based on the phenomenon of material transport. From a microscopic perspective, this phenomenon is only the staggered migration of atoms from one site in the material to another. In alloys, atoms are in constant movement, exchanging positions rapidly. These exchanges occur when two conditions are satisfied: a) There is an empty site adjacent to the atom; b) The atom must gain enough vibrational energy to break the bonds with its neighbouring atoms and, then, to cause some distortion of the lattice during its displacement [23].

Also, it is useful to describe diffusion in terms of real atomic displacements, what is equivalent to allowing a particle to develop a random walk in 2 or 3 dimensions. It is assumed that this particle has the

respective average value of any observable of the simulated system [24]. When a particle makes a two-dimensional random walk, it is assumed as follows: step sizes are equal, and movement in any direction has equal probability and is uncorrelated with previous jumps (our model deals with an isotropic and homogeneous material. However, it would be more complicated if we studied materials with a net of channels, for example). Likewise, there is a relationship between the diffusion coefficient and the random walk process described above [25].

The most important diffusion mechanisms occurring in metals are interstitial diffusion, vacancy diffusion and ring diffusion; in alloys, the dominant are the vacancy diffusion and the interstitial diffusion [26].

2.2 Model and methodology of the simulations

We will use the Kinetic Monte Carlo method, which will be detailed below. Now, we want to point out that the term *Monte Carlo method* really represent a group of computational algorithms in which the exact dynamic behaviour of any phenomenon or system is replaced by a stochastic process, i.e., the system performs random walks in the configuration space [27-28]. If the initial state is an arbitrary configuration, then each state has assigned a definite probability; besides, the system reaches equilibrium after a certain number of steps in the configuration space and the obtained average values are the ones over several configurations. The Metropolis algorithm can be used to generate samples of representative configurations, wherein the probability of occurrence of a particular configuration is proportional to the Boltzmann factor [27-28].

Usually, the Monte Carlo method is applied to molecular systems as follows: to predict average values of observables representing properties of structures in a thermal environment; to estimate the distribution of charges in molecules; and to calculate kinetic constants of a chemical reaction, free energies, dielectric constants, coefficients of compressibility, heat capacities and phase transition points, etc.

2.3 Kinetic atomistic model

We will consider a rigid BCC lattice with periodic boundary conditions, which are to avoid

border effects. Specifically, we use the B_2 structure, which is composed of two interpenetrating simple cubic sublattices, each of which has only one type of atom occupying its nodes [23].

For computational efficiency, we will use two Cartesian coordinate systems to determine the position of the nodes of the BCC lattice, which consists of N sites ($N = 2L^3$ and $L = 100$). Each coordinate system will establish the position of the nodes of each simple cubic sublattice and will be separated by the vector $a(0.5, 0.5, 0.5)$, where a is the dimension of the BCC unit cell. The binary alloy consists of N_A atoms A, N_B atoms B and one vacancy; specifically, $N = N_A + N_B + 1$ and $N_A = N_B + 1$.

Taking into account the model used, respectively, by Kim and Lim, we consider pair interaction energies between atoms located in close neighbouring sites [29-30]. These energies are symbolized ε_{XY}^i, where X and Y stand for A or B, and $i = 1$ and 2 for the NNs and the NNNs, respectively.

We will neglect phantom interactions between atoms and vacancies; these interactions are sometimes introduced to weigh up the strength of chemical bonds of the atoms having lower coordination numbers [31]. With the residence time algorithm (RTA) described below, it can be shown that the phantom interactions will not change the path of the vacancy, but only the residence (stay) time in each state. The diffusion of the A and B atoms occur by means of thermally activated exchanges of the position of the atoms (A or B) with the vacancy (V). According to the theory of rate, the frequency of an exchange X-V (where $X = A$ or B) is

$$\Gamma = \nu \exp\left\{ -\frac{\Delta E_{XV}^{\mathrm{act}}}{kT} \right\} \qquad (1)$$

where ν is the attempt-to-escape frequency [32]; k, the Boltzmann constant and T, the temperature. The E_{XV}^{act} activation energy is calculated by using the broken-bond model:

$$\Delta E_{XV}^{\mathrm{act}} = E_{\mathrm{s}} - \sum_{i=1,2} \sum_{p \in n_i(X)} \epsilon_{X_p}^i \qquad (2)$$

E_{XV}^{act} is the energy needed to extract the X-V pair from their surroundings and take the X-atom to a saddle point position, where its interaction energy with the system is E_{s} [33]. The sum in Eq. (2)

extends over all atoms in the i-th coordination sphere of the X-atom. For the sake of simplicity, we will take v and E_s as being constants. At a given temperature, the value of E_s only contributes to define the absolute time scale.

If we make $E_s = \left[(Z_1-1)(\epsilon^1_{AA}+\epsilon^1_{BB}) + Z_2(\epsilon^2_{AA}+\epsilon^2_{BB}) \right]/2$ with Z_i being the coordination number of the i-th coordination sphere, then the activation energy can be rewritten as

$$\Delta E^{\text{act}}_{XV} = \frac{1}{2} \sum_{i=1.2} \epsilon_i n^i_Y + u_i \theta_X n^i_X \qquad (3)$$

where $(X,Y) = (A,B)$ or (B,A); $\epsilon_i = \epsilon^i_{AA}+\epsilon^i_{BB}-2\epsilon^i_{AB}$ stands for the i-th ordering energy, and $u_i = \epsilon^i_{AA} - \epsilon^i_{BB}$, the i-th asymmetric energy; $\Theta_A = -1$ and $\Theta_B = 1$; n^i_X and n^i_Y are the numbers of atoms of type X and Y in the i-th coordination sphere around the site occupied by the X-atom that will be exchanged with the vacancy. Eq. (3) clearly demonstrates that not only the ordering energies but also the asymmetric energies control the kinetics of the alloy.

We assume that the attempt-to-jump frequency, v, which is derived from the theory of kinetic rate, is 1. This value does not affect any details of the kinetic Monte Carlo simulation (it simply scales the relative magnitudes of the jump amplitudes by a constant factor); however, in calculating the total simulation time (in physical seconds), it is necessary. The value of v is typically large (e.g. 10^{14} Hz) so that the approximate physical time can be obtained by dividing the number of Monte Carlo steps by 10^{14}. Since a run is 10^6, 10^7, 10^8 or 10^9 Monte Carlo steps, we can assume that the true physical time is of the order of 10^{-5}, 10^{-6}, 10^{-7} or 10^{-8} physical seconds.

At considering interactions between the NNs only, this model has been successfully used to reproduce both the kinetics of the precipitation of copper in BCC iron and the kinetics of ordering and precipitation in the B_2 structures [34-35]. With the last type of interactions, the equilibrium phase diagram of a binary alloy exhibits a second-order transition line A_2-B_2 separating two single-phase regions, and a critical temperature $T_C \sim 0.80\ \varepsilon/k$ for the $A_{50}B_{50}$ system, with $\varepsilon = \varepsilon_{AA} + \varepsilon_{BB} - 2\varepsilon_{AB}$ [36].

For the ABV alloys, as discussed here, in principle, the ordering energies need to be defined for each of the three binaries. As usual, we do not consider phantom interactions and obtain only three ordering energies ε, ε_{AA} and ε_{BB}. For compositions close to the AB binary alloy, it has been demonstrated that the thermodynamic properties are determined only by ε and the ordering energy difference, $u = \varepsilon_{AA} - \varepsilon_{BB}$, for the AV and BV binaries [35].

For practical purposes, the studied systems are so highly diluted with respect to vacancies that the effect of u on the position of the order-disorder transition line can be safely neglected. In such a case, T_C is the same as that of the AB binary alloy. In our research, with interactions up to the NNNs, our model system presents a transition between the A_2 and B_2 phases and at low temperatures, a two-phase region $A_2 + B_2$. In concordance with previous simulations of the FeAl alloy, we will use the parameters $(\varepsilon_1, \varepsilon_2, u_1, u_2) = (0.03, -0.04, -0.04, 0)$ eV [35,36]. For the $A_{50}B_{50}$ composition, T_C was found to be 1175 K.

2.4 Residence time algorithm

Since we are interested in kinetic studies, especially at low temperatures, this algorithm is appropriate for such studies [38-40]. The classical Monte Carlo algorithms are used to characterize the equilibrium properties of a system [42-43]. Nowadays, it has been demonstrated equivalence between the RTA and the Metropolis algorithm [44].

In searching to improve the computational efficiency, Young, Lanore, and Bortz et al. introduced and developed the RTAs [38,39,44]. These authors applied these procedures to explain the diffusion of vacancies, the microstructural evolution under irradiation and the Ising model with spin changes (n-foldway algorithm), respectively. In the RTAs, every attempt to reach a new configuration is successful, but the time elapsed before it occurs is not constant.

For all the corresponding computer simulations, since diffusion measurements are averaged over a very large number of vacancy jumps, we could use a variable residence time $\left(\tau_f = \frac{p+1}{Z\nu} \right)$ or a mean residence time. Thus, hereafter, we will use the latter.

3. Results and discussion

Our simulated system is similar to the FeAl alloy, which exhibits a three-phase behaviour: an ordered phase B_2, a disordered phase A_2 and a mixed phase $A_2 + B_2$. Specifically, we studied the $A_{50}B_{50}$ alloy.

The simulation space is composed of three species: the A-atoms, the B atoms, and the V vacancy. The A and B atoms can diffuse through the simulation space via interaction (or exchange movement-s) with the vacancy. To obtain a two-phase region A_2+B_2, at low temperatures, we use the interactions up to the sphere of the NNNs [36]. As mentioned above, the parameters employed are $(\varepsilon_1,\varepsilon_2,u_1,u_2)=$ (0.03,-0.04,-0.04,0) eV [35]. With these values, by using the kinetic Monte Carlo method and the grand canonical ensemble, Athènes, Bellon and Martin replicated the phase diagram of FeAl [35]. For the $A_{50}B_{50}$ composition, they found $T_C = 1175$ K as well as a tricritical temperature $T_{\text{tric}} = 690$ K.

We have used periodic boundary conditions to avoid border effects; we also consider that one type-B atom is eliminated to create one vacancy; and we also use a total number of nodes N = 2 x 10^6. All dynamics was introduced through the movement of the vacancy, and only jumps to one of the eight NNs were allowed. The degree of order of the system was monitored by means of the LRO parameter and the SRO parameter (SRO means short-range order).

In the simulation of this system, we consider that B_2 is a BCC lattice formed by two interpenetrating simple cubic sublattices α and β; the B_2 perfect order consists of the former occupied by the A-species whereas the latter, by the B species. The LRO parameter is defined thus:

$$\eta = \text{LRO} = \frac{1}{N}\left(\sum_\alpha S_i - \sum_\beta S_j\right) \quad (4)$$

where S_i and S_j are the spin variables at r_i and r_j, respectively. Likewise, S_i can take three values: +1, -1, and 0 when the i-th position of the lattice is occupied by an atom A, an atom B, or a vacancy V, respectively; the same for S_j.

To define the SRO parameter, we take a reference atom A, examine the i-th shell around it, then the p_{AB}^i probability to find different atoms B within that shell is divided by the c_B total concentration of the B atomic species. p_{AB}^i can be interpreted as the proportion of the B atoms in the i-th coordination sphere relative to an arbitrary atom A, averaged over all the A-atoms in the lattice. This parameter is known as the Warren-Cowley SRO parameter:

$$\alpha_i = 1 - \frac{p_{AB}^i}{c_B} \quad (5)$$

where $i = 1,2$. The random atomic distributions correspond to α_i null, because p_{AB}^i, the probability of finding pairs A-B, is c_B. For each temperature T we studied, it was first necessary to obtain the equilibrium state of the alloy at T. This was achieved by comparing two systems that evolved simultaneously, one of them initiating its thermalization from the completely ordered state (a perfectly ordered lattice) and the other from a completely disordered state (a lattice with a random distribution of atoms). When both systems reach the same order parameter, in particular LRO, we consider that the equilibrium state was reached at the respective temperature. Afterwards, we proceed with all convenient measurements for the alloy, which is in its macroscopic steady state. In Figures 1a and 1b, we show the earlier explained procedure for $T = 550$ K, where SRO $= \alpha_1$. This way we obtained the phase diagram in the LRO vs. T plane (Figure 2).

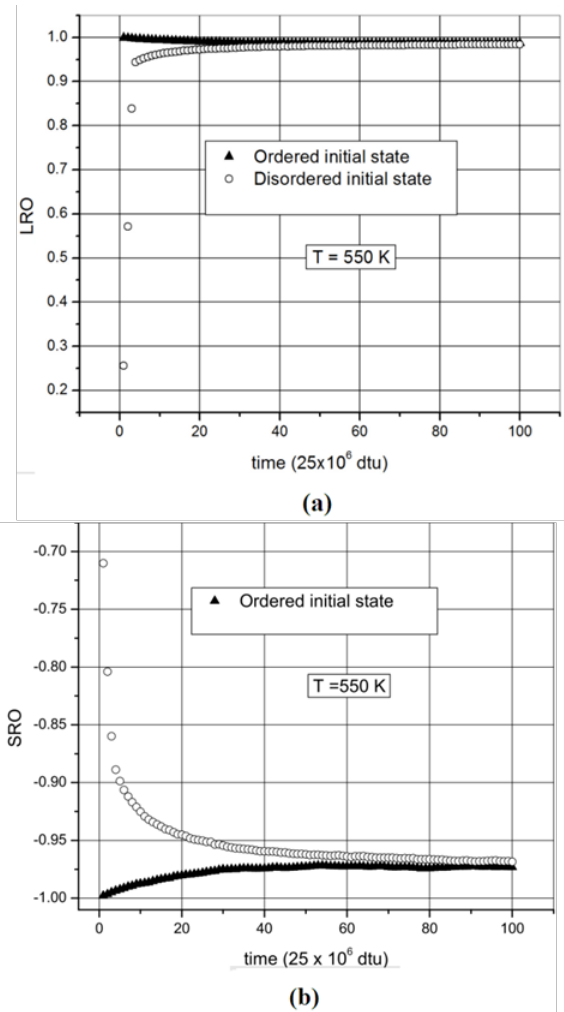**(a)**

(b)

Figure 1. Ordering process seen through the temporal evolution of the LRO and SRO order parameters.
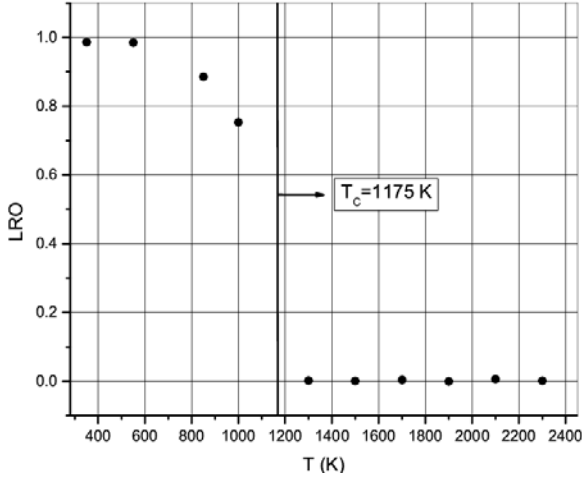
Figure 2. Phase diagram of the LRO equilibrium parameter as a function of the T temperature.

3.1 Tracer diffusion coefficient

Formally, this parameter is determined through the calculation of the mean square displacements of the tracer atoms [46]. The vacancy diffusion coefficient was calculated by

$$D_V = \lim_{t \to \infty} \left(\frac{1}{6} \frac{\partial R_V^2}{\partial t} \right) \quad (6)$$

where R_V^2 denotes the mean square displacement of the vacancy after a time t [47]. Since all the A(B) atoms can be individually viewed as tracers, the $D_{A(B)}$ tracer diffusion coefficient was calculated in the same way:

$$D_A = \lim_{t \to \infty} \left[\frac{1}{6N_A} \frac{\partial}{\partial t} \left(\sum_{\substack{\text{atoms} \\ A}} R_A^2 \right) \right] \quad (7)$$

The measured values of the mean square displacements were averaged over 60 independent simulations.

Contrary to the Metropolis standard algorithm, wherein the efficiency falls at low temperatures, with the kinetic RTA the vacancy performs a jump to a close neighbour in every attempt, i.e., in each Monte Carlo step the vacancy makes a jump. For this reason, we define the unit of time as each jump the vacancy makes and we call it dtu (dimensionless time unity).

Concerning to the mean square displacement and the autocorrelation function, there are earlier evidences that the time required to obtain measurements is inversely proportional to the temperature at which the simulation was performed

[37]. This occurs because the vacancy is trapped around a lattice node, i.e., the vacancy made reversals constituted by two consecutive jumps each other. Then, many reversals can occur around a lattice site; however, after a long time, longer when lower is the temperature, the vacancy visits another region of the alloy. Fortunately, these reversals do not happen often at moderate and high temperatures. Besides, the atomic diffusion coefficient, D_A, can be determined below and above T_C, the critical temperature; the values for $\text{Ln}(D_A)$ can be adjusted by two straight lines as a function of $1/T$ for temperatures above and below T_C; the Arrhenius graph changes its slope at T_C.

Therefore, in the Arrhenius equation $D = D_0 \exp\left(\frac{-E_A}{kT} \right)$, if we take the logarithm of both sides, we have $\text{Ln}(D) = \text{Ln}(D_0) - \left(\frac{E_A}{k} \right) \frac{1}{T}$. E. Manrique *et al.* made a least squares fitting for the Arrhenius plot ($\text{Ln}(D)$ vs. $1/T$) [37]. Specifically, they found that E_A^{act} in the ordered phase (0.42 eV) is higher than E_A^{act} in the disordered phase (0.12 eV). These values agree with experimental results [48].

In Figure 3, we show $\text{Ln}(f)$ vs. $1/T$, where f stands for the $(N-1)D_A/D_V$ ratio. The data are fitted to two straight lines above and below T_C. Over T_C, f approaches the BCC lattice correlation coefficient $f_{BCC} = 0.727$, which means that the system behaves like a conventional BCC lattice [49]. Below T_C the lower temperature, the higher values of f; besides, the values of f are greater than 1. This fact can be explained if the vacancy makes highly correlated jumps, i.e., via the 6JC. This is consistent with the results of Mishin, who found that in a system B_2, NiAl at low temperatures, the 6JC is the main responsible for the atomic migration [50].
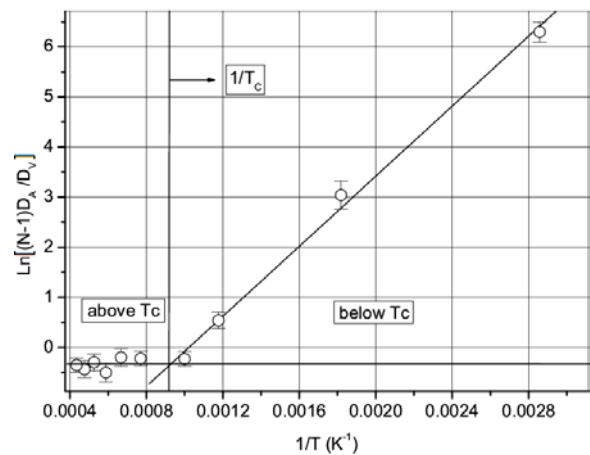

Figure 3. Arrhenius graphs of the logarithm of the ratio between atomic diffusivity and diffusivity of the vacancy vs. the inverse temperature.

3.2 Movement of the antiphase boundaries

We will also study the antiphase boundary movement in the last stages of the ordering process after quenching. The initial state is the one completely disordered at a very high temperature, in theory $T = \infty$. After quenching below T_C the long range order is developed by nucleation and growth of ordered domains. In the last stages, the system consists of a lattice of domain walls separating ordered regions.

This quenching process is shown in Figure 4, where the evolutive sequence for $T = 350$ K displays the η_i^2 field (see Eq. (11)) in the real space and the structure factor in the reciprocal space, for 1.1 x 10^6, 9.8 x 10^8 and 1.9 x 10^9 dtu. The A_2 and B_2 phases appear as dark and bright regions, respectively.

The structure factor is defined as usual

$$S_{(\vec{k},t)} = \left| \frac{1}{N} \sum_{\vec{r}} s_{(\vec{r},t)} \exp\left(i\frac{2\pi}{a}\vec{k}\cdot\vec{r} \right) \right|^2 \qquad (8)$$

To define the B_2 field of order η_i, we consider α and β to be two simple cubic sublattices required to describe the B_2 symmetry. In turn, either are subdivided into two FCC sublattices: α into α_1 and α_2, and β into β_1 and β_2. We also use the atomic occupation function

$$s_k = \begin{cases} +1 & \text{if } k \in \alpha \text{ and } k \text{ is occupied by } A. \\ +1 & \text{if } k \in \beta \text{ and } k \text{ is occupied by } B. \\ -1 & \text{else.} \end{cases} \qquad (9)$$

Around a site i, we define a cell Ω_i formed by the site itself, and its eight NNs and its six NNNs. The $\eta_i^{\nu_j}$ partial order, in a site i with respect to the ν_j sublattice, is then given by

$$\eta_i^{\nu_j} = \frac{1}{N_i^{\nu_j}} \sum_{k \in \nu_j \cap \Omega_i} s_k, \qquad (\nu = \alpha, \beta \text{ and } j = 1, 2) \qquad (10)$$

where $N_i^{\nu_j}$ is the number of sites in $\nu_j \cap \Omega_i$. Then, the B_2 field of order is defined as

$$\eta_i = \frac{1}{4} \sum_{\substack{\nu=\alpha,\beta \\ j=1,2}} \eta_i^{\nu_j} \qquad (11)$$

Besides, we consider that the S surface of the antiphase frontier, at an instant t, is proportional to $SRO_\infty - SRO_{(t)}$, which is a good approximation [51].

Since the volume of the ordered domains is roughly constant and, in a first approximation, equal to the size of the system in this regime, S is correlated with the R average domain size via $S \propto 1/R$. For a binary alloy undergoing an order-disorder transition, for the mean square displacement (R), Allen et al. proposed this law of growth:

$$R_{(t)} \propto (Mt)^x \qquad (12)$$

where $x = 1/2$ and M denotes the mobility of the antiphase boundary [52]. Then, we expect to find the following relationship:

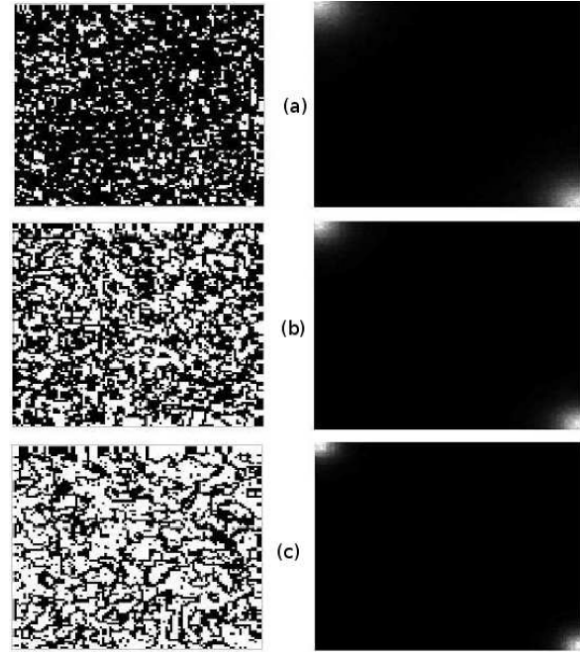$$SRO_\infty - SRO_{(t)} = Mt^{-1/2} \qquad (13)$$

Figure 4. System evolutive sequences in the real space (corresponding to a section perpendicular to (100)), left, and in the reciprocal space (in the plane (100)), right. The times are (a) 1.1 x 10^6 dtu, (b) 9.8 x 10^8 dtu, and (c) 1.9 x 10^9 dtu.

Figure 5 shows [SRO_∞ - $SRO_{(t)}$] vs. $t^{-1/2}$; therein, a linear regime is observed over a long period of time; it is higher when lower is the quenching temperature and is interpreted as the growth regime (coarsening). The fitting line for this regime obviously goes through the origin when $t \to \infty$. Since all points not belonging to the coarsening regime are on the fitting line for the regime, then we will calculate the mobility of the minimum value of [SRO_∞ - $SRO_{(t)}$]$t^{1/2}$. Consequently, for 350 K, in Figure 6a we have [SRO_∞ - $SRO_{(t)}$] vs. $t^{1/2}$ and in

Figure 6b, the minimum value used for calculating the mobility of the antiphase boundary as a function of $t^{-1/2}$, too.

In Figure 6b, the obtained values result from the average of 60 independent simulations; we exclude the very low values of the equilibrium LRO parameter, what is typical of systems having competing domains.

Figure 7 shows the Arrhenius graph of Log(M) vs. $1/T$. The temperature range is restricted to values lower than T_C because the antiphase boundaries only exist for these values. We found out that the activation energy for the movement of the antiphase boundaries is 0.17 eV. This small value is explained if the vacancy is restricted to moving mainly in disordered regions; so, there is no significant change in its environment before and after the jump, therefore, it does not need much energy for its migration. In short, the vacancy moves mainly around the antiphase boundaries, which are disordered regions.
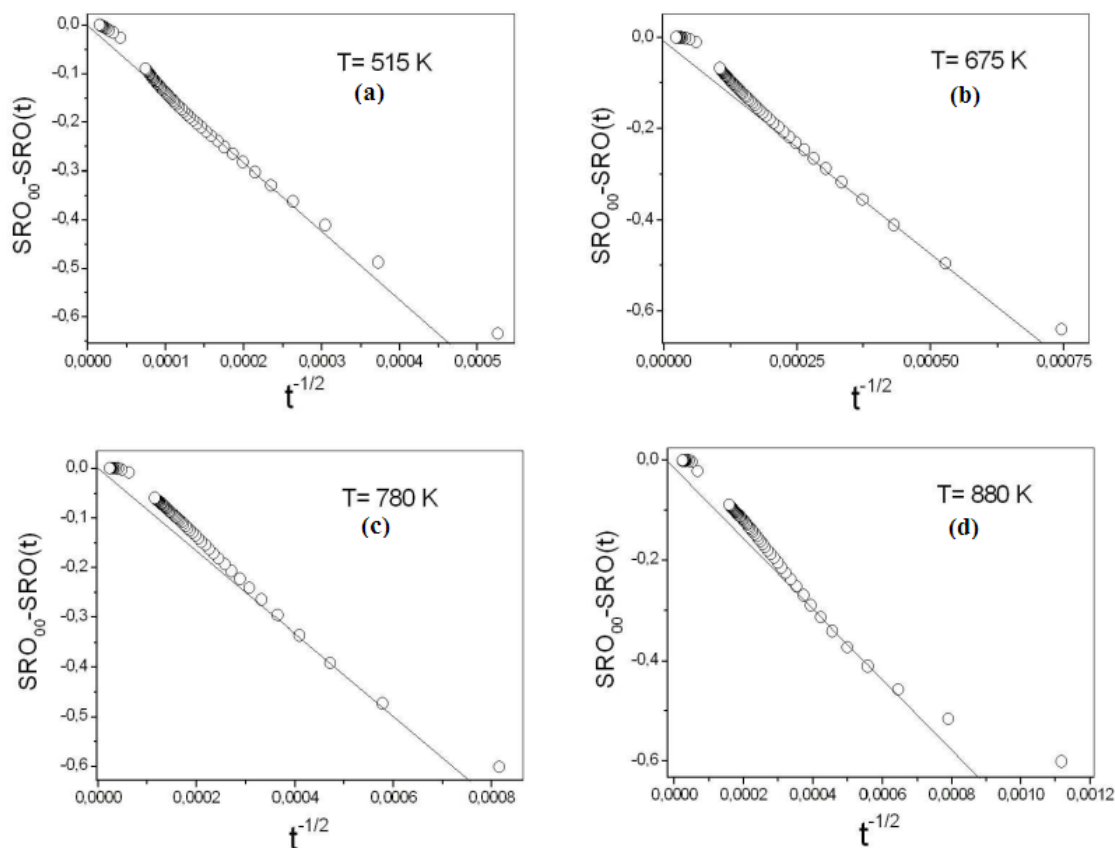

Figure 5. Deviation of the SRO parameter from its equilibrium value vs. $t^{-1/2}$, for various temperatures.
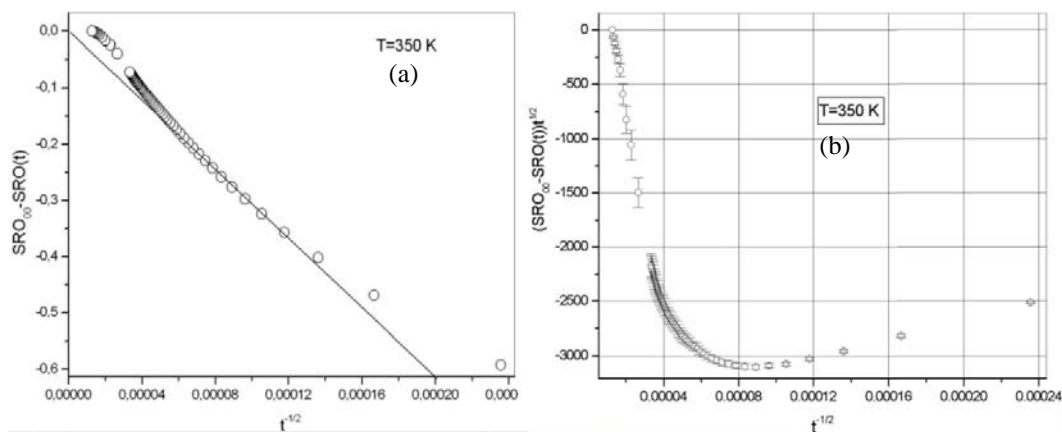

Figure 6. At 350 K, (a) deviation of the SRO parameter from its equilibrium value vs. $t^{-1/2}$; (b) Minimum value of [$SRO_\infty - SRO_{(t)}$] averaged over 60 independent simulations.
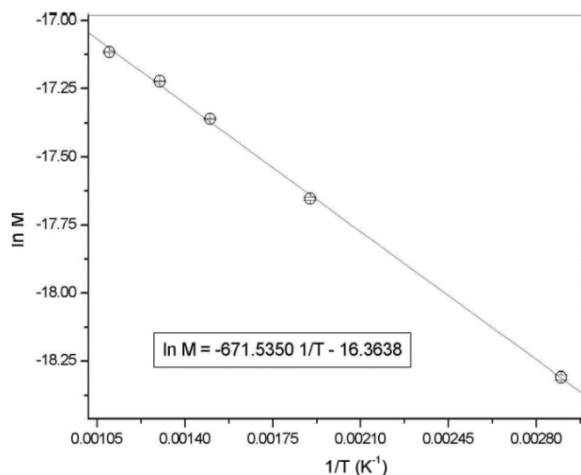
Figure 7. Arrhenius graphs of the logarithm of mobility vs. the inverse temperature.

3.3 Measurement of the autocorrelation function

Whereas the tracer diffusion experiments allow indirect evidence on elementary diffusion jumps [53], direct evidence can be obtained from QEMS, quasi-elastic neutron scattering, and forward-scattered resonant synchrotron radiation [54-56]. These experiments typically measure the autocorrelation function of a labelled atom in the alloy.

The autocorrelation function, after a time t, gives information of a labelled atom initially located at the origin. It has recently been inferred from QEMS experiments for the type- B_2 alloy FeAl that the iron atoms actually jump between nodes of their own sublattice [57-58]. These jumps are mostly to the next-next-nearest neighbours (NNNNs) and partly to the NNNs. At intermediate temperatures, QEMS also provides evidence that the jumps are a combination of two jumps to the NNs.

Figure 8 shows the probability of finding an atom A, located at the origin in $t = 0$, in the n-th coordination sphere in a time t. In the simulation, since the program source code monitors the displacement vector of all the atoms, including the vacancy, at each t, the autocorrelation function is a function of time. Then, to obtain the autocorrelation function, we count the atoms of the same type (A or B) with equal total displacement (with the same modulus of the displacement vector), i.e. the atoms within the same coordination sphere.

Also in Figure 8, it is observed that after a time of 3 x 10^9 dtu, 90% of the A-atoms did not move, or if they did so, they finally returned to their starting point (the corresponding origin of coordinates); this because, by definition, all the A-atoms are located

in the shell zero at $t = 0$ dtu. The first coordination sphere is empty, meanwhile the remaining 10% of the A-atoms are hosted in the second and third shells of closer neighbours. This fact is important because 10% of the A-atoms move through the 6JC (after the 6JC has been completed, the crystal is again ordered and the vacancy has migrated to a NNN or a NNNN). Therefore, at $T = 350$ K, 10% of atoms A have performed at least one 6JC. This conclusion is supported by Mishin, who using computational simulation found that, at low temperatures, the 6JC is the main responsible of the atomic migration in the NiAl alloy [50]. Furthermore, according to Figure 8, there is a preference for jumps to the NNNs over the jumps to NNNNs, with a relative probability 2, which is independent of time, after $t = 1.5$ x 10^9 dtu.
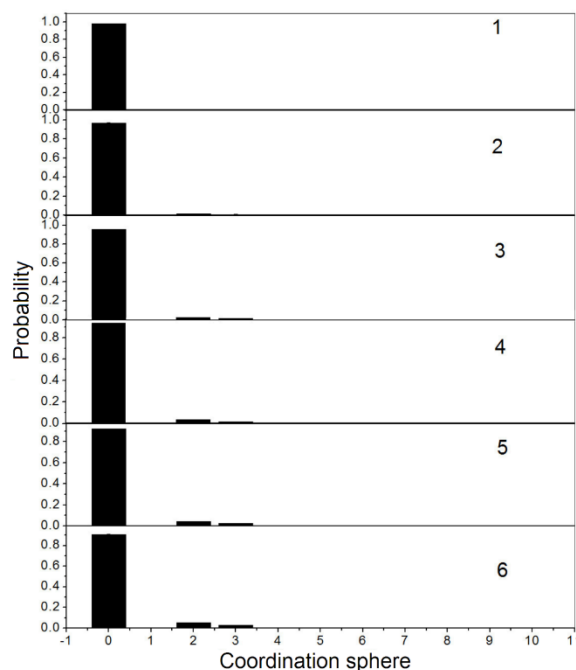

Figure 8. Autocorrelation function of the A-atoms, in several times at 350 K. Numbers 1, 2, ..., 6 indicate time instants τ, 2τ, ..., 6τ, respectively, where $\tau = 5$ x 10^8 dtu.

Since the first coordination sphere is empty all time and, on the contrary, the second and third coordination sphere are always occupied, then there are two possibilities: 1) the vacancy performs the 6JC; 2) the vacancy jumps to the NNNs or to the NNNNs.

From the aforementioned QEMS experiments of B_2-FeAl, we conclude that the (iron) A-atoms jump to sites of their own sublattice (to the NNNs and NNNNs shells), via the combination of 2 jumps to the NNs. Consequently, an iron atom occupies for a brief time an antistructure site in the sublattice of aluminium.
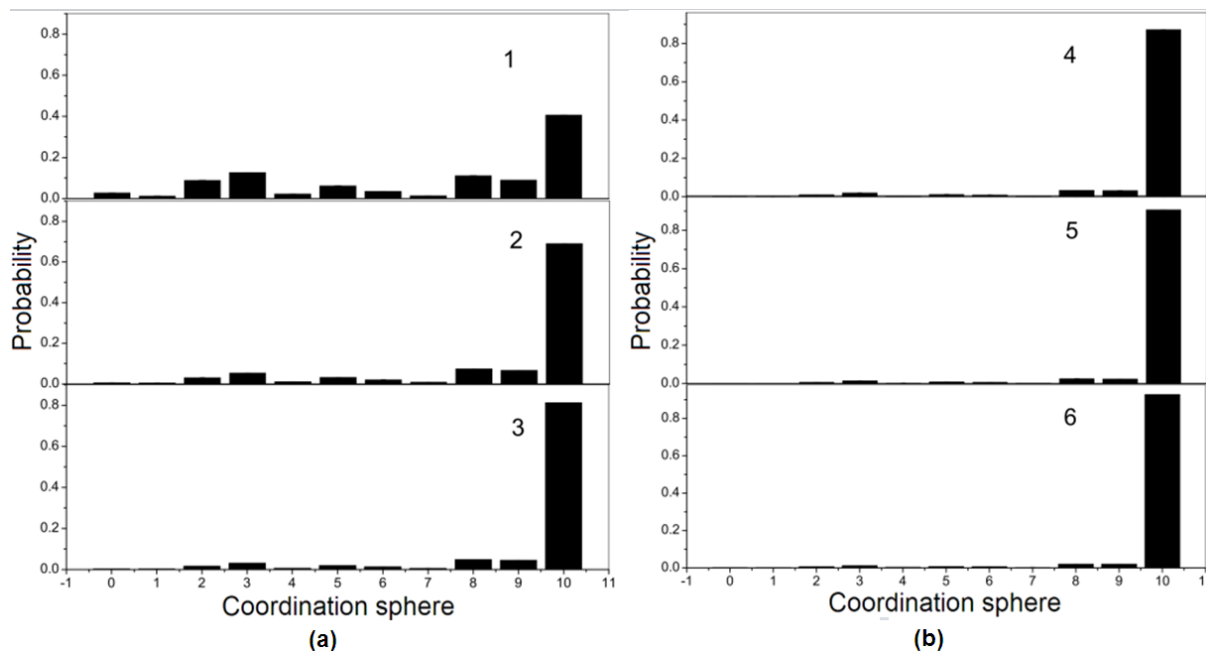
Figure 9. Autocorrelation function of the A-atoms, at various times at 850 K. Measurements were taken after time intervals of 5 x 10^7 dtu.

In Figure 9a, we have the autocorrelation function of the A-atoms at different times at 850 K and in which measurements were taken after each 5 x 10^7 dtu; therein, we observe that the A-atoms jump to sites of their own sublattice (to the second and third shells of closer neighbours) via the combination of 2 jumps to the NNs. It results in a brief time of occupation of an antistructure site in the aluminium sublattice. We arrive at this conclusion by means of the same reasoning performed for the autocorrelation function of the A-atoms for $T = 550$ K. However, this behaviour corresponds to a very small fraction of the A-atoms, which decreases over time; in the final stage, this fraction becomes, after 1.5 x 10^8 dtu, around 4.5% of all the A-atoms. Besides, 95% of the A-atoms have migrated to the eighth or greater coordination spheres.

In Figure 9b, we observe that the A-atoms carry out practically random walks, i.e. the vacancy visits each region of the lattice with the same frequency, and its movements are uncorrelated or very low correlated, i.e., there are no jumps of the vacancy by the 6JC. After $t = 3$ x 10^8 dtu, almost 100% of the A-atoms have migrated to the eight or greater coordination spheres.

4. Conclusions

To indirectly obtain information on atomic diffusion, we have used the measurement of the total mean quadratic displacement of the iron atoms in the FeAl alloy. Likewise, despite the residence time algorithm is more efficient than the Metropolis algorithm at very low temperatures, it was not efficient enough. This because, at these temperatures, it was necessary to use more simulation time to measure the mean square displacements. What can be explained by the fact that, at very low temperatures, the vacancy along its trajectory returned to the initial node from which it jumped to the next node; this phenomenon we call it reversion and occurred repeatedly involving the initial node. Reversion occurred throughout the volume of the model alloy during the displacement of the vacancy in the alloy. However, this was not the case at moderate and high temperatures; so, we conclude that the residence time algorithm is very efficient for these last temperatures.

The movement of the antiphase boundaries, during the last stages of the ordering process, was also studied. The excess energy of the alloy was concentrated at the antiphase boundaries, what is due to the fact that the vacancy moves, most of the time, in the disordered regions, i.e., around the antiphase boundaries. Finally, we studied the autocorrelation function of the type-A atoms, what gives information of the position in time of a tagged atom. This function provides information, in a direct way, on elemental atomic jumps during diffusion; we found three regimes of atomic jumps. At low temperatures the main mechanism of diffusion is the 6JC. At moderate temperatures, the diffusion mechanism of the type-A atoms is the jump between positions within the sublattice, to the second or third coordination sphere; however, these jumps are not direct but by means of the combination of two consecutive jumps to closer neighbours. At high temperatures, but below and close to T_C the main mechanism of diffusion is that in which the vacancy performs low correlated jumps, random walks, during its migration in the crystal.

5. Acknowledgments

References

[1] J. K. Tien and J. Caulfield, *Superalloys, Supercomposites and superceramics*, Boston: Academic Press Inc., 1989.

[2] G. Bester, B. Meyer, M. Fahnle, and C. L. Fu, "Dominant thermal defects in B2FeAl," *Materials Science and Engineering: A,* vol. 323, pp. 487-490, 2002.

[3] T. Haraguchi and M. Kogachi, "Point defect behavior in B2-type intermetallic compounds," *Materials Science and Engineering: A,* vol. 329331, pp. 402-407, 2002.

[4] R. Nakamura, K Takasawa, Y Yamazaki, and Y. Iijima, "Single-phase interdiffusion in the B2 type intermetallic compounds NiAl, CoAl and FeAl," *Intermetallics,* vol. 10, pp. 195-204, 2002.

[5] O. Semenova, R. Krachler, and H. Ipser, "A generalized defect correlation model for B2 compounds," *Solid State Sciences*, vol. 10, pp. 1236-1244, 2008.

[6] A. Hanc, J. Kansy, G. Dercz, and I. Jendrzejewska, "Point defect structure in B2-ordered FeAl alloys," *Journal of Alloys and Compounds*, vol. 480, pp. 84-86, 2009.

[7] R. Felwish, G. Vogl, and B. Sepiol, "Elementary diffusion jump of iron atoms in intermetallic phases studied by Mossbauer spectroscopy II. From order to disorder," *Acta Metallurgica et Materialia*, vol. 43, pp. 2033-2039, 1995.

[8] B. Sepiol, "Mössbauer Spectroscopy in Diffusion Studies", *Defect and Diffusion Forum*, vol. 125-126, pp. 1-18, 1995.

[9] G. Vogl and B. Sepiol, "Elementary diffusion jump of iron atoms in intermetallic phases studied by Mossbauer spectroscopy I. FeAl close to 450 equiatomic stoichiometry," *Acta Metallurgica et Materialia,* vol. 42, pp. 3175-3181, 1994.

[10] A. T. Donaldson and R. D. Rawlings, "The diffusion of nickel and gallium in the intermetallic compound NiGa," *Acta Metallurgica*, vol. 24, pp. 285-291, 1976.

[11] A. Lutze-Birk and H. Jacobi, "Diffusion of 114mIn in NiAl," *Scripta Metallurgica*, vol. 9, pp. 761-765, 1975.

[12] H. Hahn, G. Frohberg, and H. Wever, "Self diffusion in the intermetallic B_2 electron compound PdIn," *Physica Status Solidi (a),* vol. 79, 559-565, 1983.

[13] P. Wynblatt, "Diffusion mechanisms in ordered body-centered cubic alloys," *Acta Metallurgica,* vol. 15, pp. 1453-1460, 1967.

[14] E. W. Elcock and C. W. McCombie, "Vacancy Diffusion in Binary Ordered Alloys," *Physical Review,* vol. 109, pp. 605, 1958.

[15] C. R. Kao and Y.A. Chang, "On the composition dependencies of self-diffusion coefficients in B2 intermetallic compounds," *Intermetallics,* vol. 1, pp. 237-250, 1993.

[16] N. A. Stolwijk, M. Van Gend and H. Bakker, "Self-diffusion in the intermetallic compound CoGa," *Philosophical Magazine A,* vol. 42, pp. 783-808, 1980.

[17] J. L. Jordan and S. C. Deevi, "Vacancy formation and effects in FeAl," *Intermetallics,* vol. 11, pp. 507-528, 2003.

[18] J. H. Schneibel and L. M. Pike, "A technique for measuring thermal vacancy concentrations in stoichiometric FeAl," *Intermetallics,* vol. 12, pp. 85-90, 2004.

[19] M. Athènes, P. Bellon and G. Martin, "Identification of novel diffusion cycles in B2 ordered phases by Monte Carlo simulation," *Philosophical Magazine A,* vol. 76, pp. 565-585, 1997.

[20] J. Kärger and D. M. Ruthven, "Diffusion in nanoporous materials: fundamental principles, insights and challenges," *New Journal of Chemistry*, vol. 40, pp. 4027, 2016.

[21] J. Kärger, D. M. Ruthven and D. N. Theodorou, *Diffusion in Nanoporous Materials Volume 1 & 2*, 1st Edition, US: Wiley-VCH, 2012.

[22] B. Tuck, *Introduction to Diffusion in Semiconductors* (IEE Monograph Series vol. 16), UK.: Peter Peregrinus Ltd., 1974.

[23] E. V. Manrique Castillo, "Simulación Monte Carlo de la transición orden-desorden y la formación de agregados atómicos en las aleaciones modelos tridimensionales," in Licentiate Thesis, Lima, Peru, 2006.

[24] R. J. Borg and G. J. Dienes, *An Introduction to Solid State Diffusion*, Boston: Academic Press, 1988.

[25] P. G. Shewmon, *Diffusion in Solids*, US: McGraw-Hill Book Co., 1963.

[26] E. V. Manrique Castillo, "Simulación Monte Carlo Cinético de la Difusión Atómica en la Aleación FeAl", MSc. Thesis, UNMSM, Lima, Peru, 2014.

[27] K. Binder, *Monte Carlo Methods in Condensed Matter*, Berlin 495: Springer, 1992.

[28] J. M. Hammersley and D. C. Handscomb, *Monte Carlo Methods*, New York: Wiley, 1967.

[29] S. M. Kim, "Vacancy properties in ordered CoGa and FeAl," *Journal of Physics and Chemistry of Solids,* vol. 49, vol. 65-69, 1988.

[30] S. H. Lim, G. E. Murch, and W. A. Oates, "Configurational thermodynamics of vacancy formation in solids by Monte Carlo simulation," *Journal of Physics and Chemistry of Solids,* vol. 53, pp. 175-180, 1992.

[31] M. Doyama and J. S. Koehler, "Relation between the formation energy of a vacancy and the nearest neighbor interactions in pure metals and liquid metals," *Acta Metallurgica*, vol. 24, pp. 871-879, 1976.

[32] C. P. Flynn, *Point and Defects Diffusion*, Oxford: Clarendon Press, 1972.

[33] G. Martin, "Atomic mobility in Cahn's diffusion model," *Physical Review B*, vol. 41, pp. 2279, 1990.

[34] F. Soisson, A. Barbu, and G. Martin, "Monte Carlo simulations of copper precipitation in dilute iron-copper alloys during thermal ageing and under electron irradiation," *Acta Metallurgica,* vol. 44, pp. 3789-3800, 1996.

[35] M. Athènes, P. Bellon, and G. Martin, "A Monte-Carlo study of B2 ordering and precipitation via vacancy mechanism in b.c.c. lattices," *Acta Metallurgica,* vol. 44, pp. 4739-4748, 1996.

[36] H. Ackermann, G. Inden, and R. Kikuchi, "Tetrahedron approximation of the cluster variation method for b.c.c. alloys," *Acta Metallurgica,* vol. 37, pp. 1-7, 1989.

[37] E. V. Manrique Castillo, J .Rojas Tapia, and E. Torres Tapia, "Estudio de la difusión atómica en el intermetálico FeAl mediante Monte Carlo cinético," *Revista de Investigación de Física UNMSM* 14, pp. 1-7, 2011.

[38] W. Young and E. Elcock, "Monte Carlo studies of vacancy migration in binary ordered alloys: I," *Proceedings of the Physical Society,* vol. 89, pp. 735-746, 1966.

[39] J. L. Bocquet, Report CEA-R4565, Commissariat à l'Energie Atomique, Gif-sur-Yvette, 1974.

[40] A. B. Bortz, M. H. Kalos, and J. L. Lebowitz, "New algorithm for Monte-Carlo simulations of Ising spin systems," *Journal of Computational Physics,* vol. 17, pp. 1018, 1975.

[41] F. Haider, "Monte Carlo Study of the Phase Stability of Ordered FCC Phases Under Irradiation" IN: *Ordering and Disordering in Alloys,* edited by A. R. Yavari, Amsterdam: Elsevier, 1992.

[42] G. S. Fishman, *Monte Carlo: Concepts, Algorithms, and Applications*, New York: Springer Verlag Inc., 1996.

[43] H. Gould and J. Tobochnik, "Overcoming Critical Slowing Down," *Computers in Physics,* vol. 3, p. 82, 1989.

[44] M. A. Novotny, "A new approach to an old algorithm for the Simulation of Ising-like Systems," *Computer in Physics*, vol. 9, p. 46, 1995.

[45] J. M. Lanore, Report CEA-N4565, Commissariat à l'Energie Atomique, Gif-sur-Yvette, 1972.

[46] H. Bakker, N. Stolwijk, L. P. Van der Meij and T. J. Zuurendonk, "Microstructural dependence of vacancy diffusion in ordered alloys," *Nuclear Metallic, Metallic Society AIME (US)*, vol. 20, p. 96, 1976.

[47] L. Zhao, R. Najafabadi, and D. J. Srolovitz, "Determination of vacancy and atomic diffusivities in solid solution alloys," *Acta Metallurgica,* vol. 44, pp. 2737-2749, 1996.

[48] Y. W. Cui, R. Kato, T. Omori, I. Ohnuma, K. Oikawa, R. Kainuma, and K. Ishida, "Revisiting diffusion in FeAl intermetallics: Experimental determination and phenomenological treatment," *Scripta Materialia*, vol. 62, 189-197, 2010.

[49] H. Mehrer, *Computer Simulation of Liquids,* Berlin: Springer-Verlag, 2007.

[50] Y. Mishin and D. Farkas, "Atomistic simulation of point-defects and diffusion in B2 NiAl. Part II. Diffusion mechanisms," *Philosophical Magazine A,* vol. 75, pp. 187-199, 1997.

[51] M. K. Phani, J. L. Lebowitz, M. H. Kalos, and O. Penrose, "Kinetics of an Order-Disorder Transition," *Review Letters*, vol. 45, pp. 366, 1980.

[52] S. M. Allen and J. W. Cahn, "A microscopic theory for antiphase boundary motion and its application to antiphase domain coarsening," *Acta Metallurgica*, vol. 27, pp. 1085-1095, 1979.

[53] H. M. Eggersman, B. Sepiol, G. Vogl, and H. Mehrer, "Diffusion in the Intermetallic Phases of the Fe-Al system studied by Tracer and Mössbauer Techniques," *Defect and Diffusion Forum,* vol. 143-147, pp. 339, 1997.

[54] G. Vogl, *Mossbauer Spectroscopy Applied to Magnetism and Materials Science Vol. 2,* New York: Plenum Press, 1996.

[55] M. Bée, *Quasielastic Neutron Scattering,* Bristol: Adam Gilger, 1988.

[56] B. Sepiol, A. Meyer, G. Vogl, R. Ruffer, A. I. Chumakov, and A. Q. R. Baron, "Time Domain Study of ^{57}Fe Diffusion using Nuclear Forward Scattering of Synchrotron Radiation," *Physical Review Letters*, vol. 76, pp. 3220, 1996.

[57] G. Vogl and B. Sepiol, "Elementary diffusion jump of iron atoms in intermetallic phases studied by Mossbauer spectroscopy I. FeAl close to equiatomic stoichiometry," *Acta Metallurgica et Materialia,* vol. 42, 3175-3181, 1994.

[58] B. Sepiol, C. Czihak, A. Meyer, G. Vogl, J. Metge, and R. Rüffer, "Synchrotron radiation study of diffusion in FeAl," *Hyperfine Interactions,* vol. 113, pp. 449-454, 1998.